JOURNAL OF MATERIALS SCIENCE **36** (2001) 4961 – 4967

Mechanical and elastic properties of transparent nanocrystalline TeO_2-based glass-ceramics

F. TORRES, Y. BENINO, T. KOMATSU*
Department of Chemistry, Nagaoka University of Technology, Nagaoka 940-2188, Japan
E-mail: komatsu@chem.nagaokaut.ac.jp

C. LAVELLE
Departamento de Ingeniería de los Materiales, Universidad Simón Bolívar, Sartenejas, Edo Miranda, Venezuela

Mechanical and elastic properties of transparent TeO_2-based glass-ceramics ($15K_2O \cdot 15Nb_2O_5 \cdot 70TeO_2$) consisting of nanocrystalline particles (each particle size: 40–50 nm) and showing optical second harmonic generation were evaluated by means of usual Vickers indentation and nanoindentation tests. The precursor glass has Vickers hardness H_v of 2.9 GPa, Young's modulus E of 54.7 GPa, the fracture toughness K_c of 0.25 $MPam^{1/2}$ and Poisson's ratio of 0.24. The transparent nanocrystalline glass-ceramic heat-treated at 420°C for 1 h has $H_v = 3.8$ GPa, $E = 75.9$ GPa and $K_c = 0.34$ $MPam^{1/2}$, and the opaque glass-ceramic heat-treated at 475°C for 1 h has $H_v = 4.5$ GPa, $E = 82.9$ GPa and $K_c = 0.68$ $MPam^{1/2}$, demonstrating that poor mechanical and elastic properties of the precursor TeO_2-based glass are improved through sufficient crystallization. The fracture surface energy, brittleness and elastic recoveries (about 44%) after unloading (the maximum load: 30 mN) of transparent nanocrystalline glass-ceramics are almost the same as those of the precursor glass, implying that the interaction among nanocrystalline particles is not so strong.

1. Introduction

Tellurium oxide (TeO_2) based glasses are scientific and technical interest on account of their low melting temperatures, high refractive indices, high dielectric constants and good infrared transmission and recently have been considered as promising materials for use in optical amplifiers or nonlinear optical devices [1, 2]. Very recently, Watanabe *et al*. [3] measured the temperature dependence of Vickers hardness of TeO_2-based glasses such as $15Na_2O \cdot 15ZnO \cdot 70TeO_2$ from room temperature to the glass transition region and demonstrated that TeO_2-based glasses are largely fragile, i.e. crack formation under indenter easily occurs, the Vickers hardness at room temperature is around 3 GPa and the hardness decreases sharply in the glass transition region. For technical applications of such attractive TeO_2-based glasses, it is important to improve their poor mechanical properties. On the other hand, optically transparent TeO_2-based glass-ceramics consisting of nanocrystalline particles around 20–50 nm have been successfully prepared, and it has been reported that such transparent glass-ceramics show more attractive optical properties such as second harmonic generation (SHG) or strong upconversion fluorescence compared with precursor TeO_2-based glasses [4–7]. It is of interest and important to clarify mechanical and elastic properties of TeO_2-based glass-ceramics for technical applications of such transparent nanocrystalline glass-ceramics.

In this study, we focus our attention on transparent glass-ceramics with a nominal composition of $15K_2O \cdot 15Nb_2O_5 \cdot 70TeO_2$, because its precursor glass crystallizes easily and also transparent nanocrystalline glass-ceramics are easily obtained [4–7]. Some mechanical and elastic properties such as Vickers hardness, fracture toughness, brittleness and Young's modulus at room temperature were measured, and their features for transparent nanocrystalline TeO_2-based glass-ceramics were clarified.

2. Experimental procedure

The glass with a nominal composition of $15K_2O \cdot 15Nb_2O_5 \cdot 70TeO_2$ was prepared using a conventional melt-quenching method. Commercial powders of reagent grade K_2CO_3, Nb_2O_5 and TeO_2 were mixed and melted in a platinum crucible at 1000°C for 30 min in an electric furnace. The melt was poured in an alumina mold over an iron plate heated at 200°C to reduce breakage from thermal shock. The glass was annealed at 370°C to eliminate internal stress in the glass. The glass transition temperature T_g and crystallization onset temperature T_x were determined using differential thermal analysis (DTA) at a heating rate of 10 K min^{-1}.

*Author to whom all correspondence should be addressed.

The glass with $T_g = 369°C$ was converted into glass-ceramics through the so-called two-step heat-treatment in order to obtain good optical transparency. The first heat-treatment temperature was 369°C and the period was 1 h. The second heat-treatment temperatures and period were 400–475°C and 1 h. The heating rate was 5 K min^{-1}.

The crystalline phase present in the heat-treated samples were examined by X-ray diffraction (XRD) analyses at room temperature using Cu K_α radiation. The glass and heat-treated samples were mechanically polished to get mirror surface using CeO_2 powders for measurements of mechanical and elastic properties. Vickers hardness, H_v, at room temperature was measured using Akashi HM-114 in air (relative humidity was 64%). The applied loads were in the range of 245–980 mN, and the time of loading was 15 s. The Young's modulus and the fraction of elastic recovery during unloading were also evaluated using a Fischer H-100 ultra low-load microhardness indenter designed by Fischer Co. at room temperature. A diamond Vickers indenter tip was used with a geometrical correction procedure for accurate calculation of hardness. The load was applied to 30 mN and then the applied load was decreased to 0 mN. Measurements for each sample were carried out ten times under the same measuring condition.

3. Results and discussion

Firstly, it would be worth to summarize the main conclusions for the crystallization of $15K_2O \cdot 15Nb_2O_5 \cdot 70TeO_2$ glass (hereafter designated as Base glass) reported in previous papers [4, 5]: 1) the formation of two different crystalline phases are observed in the glass-ceramics, 2) the initial crystalline phase (hereafter phase I) has a disordered fluorite-type structure, 3) phase I might be metastable, because it is not formed in a powder sintering method but is formed through a crystallization of tellurite glasses, 4) transparent glass-ceramics consisting of phase I have been successfully prepared and show SHG, 5) phase I disappears at high temperatures and a new crystalline phase (hereafter phase II) is formed, 6) glass-ceramics consisting of phase II are opaque and the crystal structure of phase II has not been clarified at this moment. The DTA pattern for Base glass is shown in Fig. 1, and the exothermic peaks corresponding to the formations of phase I and phase II are marked in the figure. The XRD powder patterns for the glass-ceramics obtained by various heat-treatments at 400–475°C for 1 h are shown in Fig. 2, indicating that the glass-ceramics obtained by heat-treatments at 400–440°C consist of phase I and the transformation of phase I to phase II occurs at around 450°C.

3.1. Vickers hardness

From deformation-fracture patterns in Vickers indenter tests, the values of Vickers hardness, H_v, for Base glass and glass-ceramics of $15K_2O \cdot 15Nb_2O_5 \cdot 70TeO_2$ were evaluated using Equation 1:

$$H_v = \frac{P}{\alpha_0 a^2} \quad (1)$$

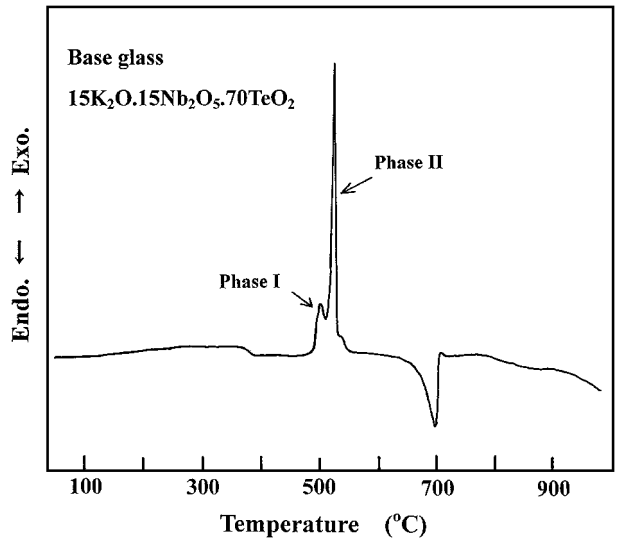

Figure 1 DTA pattern for $15K_2O \cdot 15Nb_2O_5 \cdot 70TeO_2$ glass. Heating rate was 10 K min^{-1}.

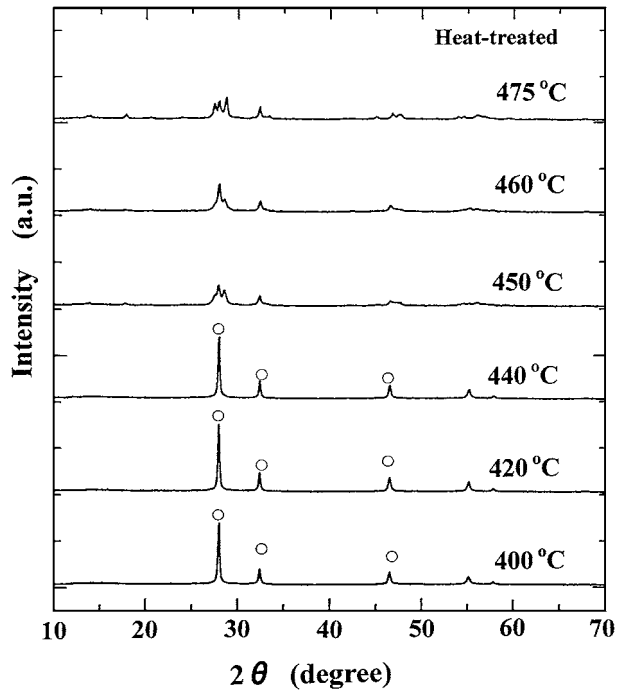

Figure 2 XRD powder patterns at room temperature for the glass-ceramics ($15K_2O \cdot 15Nb_2O_5 \cdot 70TeO_2$) obtained by heat-treatments at 400–475°C for 1 h. ◯ : phase I.

where P is an applied load, a is a characteristic indentation diagonal and α_o is an indenter constant of 2.157 in the present experiment used a diamond pyramid indenter. It was confirmed that the relation between P (245–980 mN) and a given by Equation 1, i.e. $a \propto P^{1/2}$, is well hold in the present samples. From the scanning electron micrographs of indentation patterns, it was also confirmed that Vickers-produced fracture patterns for the samples were penny-like radial/median cracks. The evaluated values of Vickers hardness at room temperature in air are shown in Table I and Fig. 3. The precursor glass has $H_v = 2.9$ GPa, transparent glass-ceramics consisting of phase I have around $H_v = 3.8$ GPa, and opaque glass-ceramics consisting of phase II have $H_v \geqq 4.3$ GPa. Although the Vickers hardness increases gradually with increasing heat-treatment

TABLE I Values of Vickers hardness H_v, Young's modulus E, fracture toughness K_c, fracture surface energy γ_f and brittleness $B(I)$ and $B(II)$ for $15K_2O \cdot 15Nb_2O_5 \cdot 70TeO_2$ glass and glass-ceramics.

Sample	H_v (GPa)	E (GPa)	K_c (MPam$^{1/2}$)	γ_f (Jm^{-2})	$B(I)$ (μm$^{-1/2}$)	$B(II)$ (μm$^{-1/2}$)
Glass	2.9	54.7	0.25	0.5	11.7	11.6
Heat-treated						
400°C, 1 h	3.3	77.8	0.40	1.0	8.3	8.3
420°C, 1 h	3.8	75.9	0.34	0.7	11.3	11.3
440°C, 1 h	3.8	74.4	0.28	0.5	13.6	13.6
450°C, 1 h	3.8	71.6	0.31	0.6	12.3	12.4
460°C, 1 h	4.3	75.9	0.43	1.1	10.1	10.1
475°C, 1 h	4.5	82.9	0.68	2.6	6.6	6.6

B(I) was estimated using Equation 7 and B(II) was calculated using Eq. (8) with $\gamma = 18$.

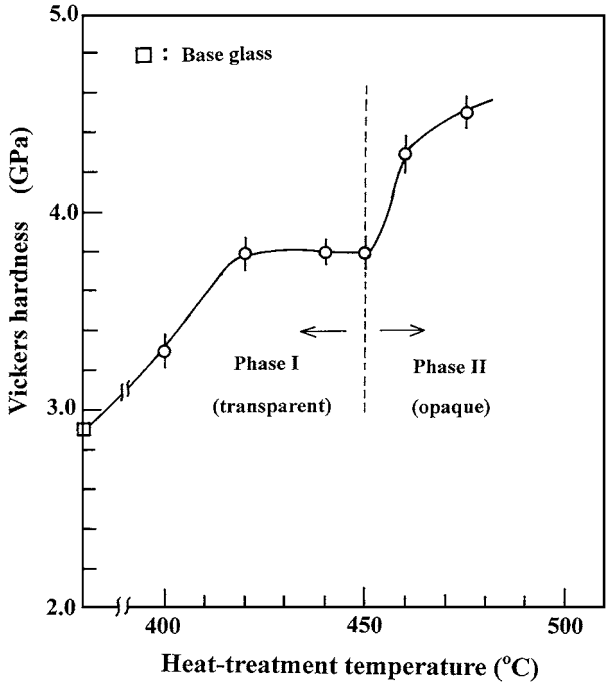

Figure 3 Vickers hardness at room temperature for the Base glass and glass-ceramics ($15K_2O \cdot 15Nb_2O_5 \cdot 70TeO_2$) obtained by heat-treatments at 400–475°C for 1 h.

temperature, its behavior is not monotonous. That is, the change in H_v is closely related to not only the formation of phase I but also to the transformation from phase I to phase II.

The diameter of each crystalline particles in transparent glass-ceramics was estimated from the full width at the half maximum of an X-ray diffraction peak at around $2\theta = 28°$ by using Scherrer's equation. The estimated diameters were 40–50 nm. The densities of Base glass, transparent glass-ceramics (heat-treated at 400–435°C) and opaque glass-ceramic (heat-treated at 475°C) are 4.66, 4.95–4.97 and 5.08 g cm^{-3} , respectively [4], meaning that the glass-ceramics have more dense atom packing structures compared with the precursor glass. The thermal expansion coefficients of Base glass and transparent glass-ceramics in the temperature range of 50–350°C are 156×10^{-7} and 124×10^{-7} K^{-1}, respectively [8]. This suggests that bond strengths among constituents atoms in transparent glass-ceramics would become more strong compared with the precursor glass, although each crystalline particle is nanosize. Such changes in atom packing structures and bond strengths might be the reason for the increase in the Vickers hardness shown in Fig. 3.

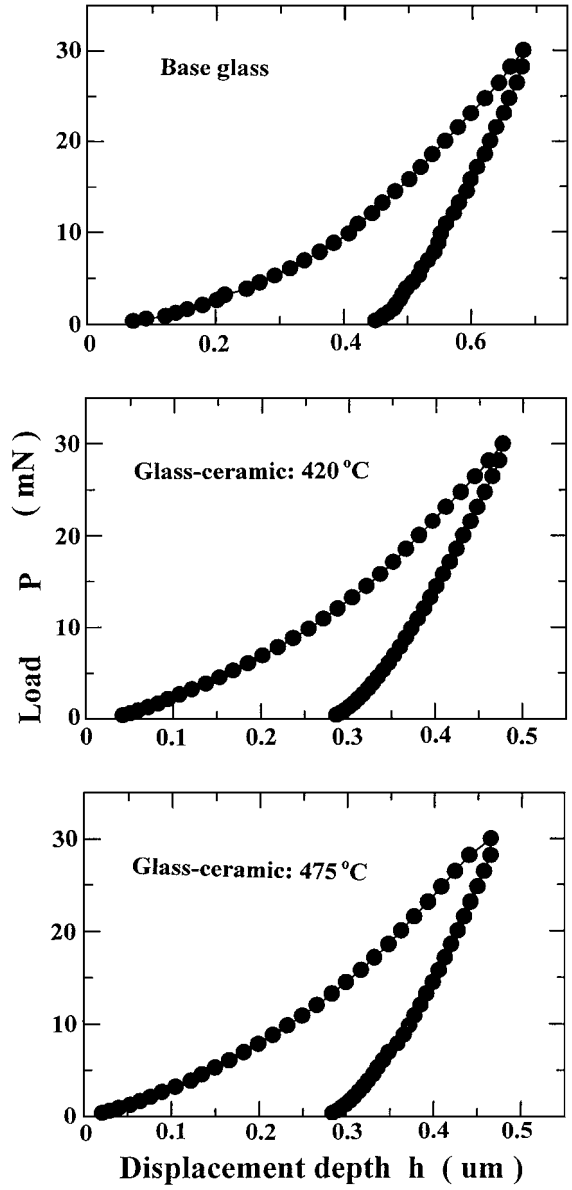

Figure 4 Indenter load versus indenter displacement at room temperature for the Base glass and glass-ceramics ($15K_2O \cdot 15Nb_2O_5 \cdot 70TeO_2$) obtained by heat-treatments at 420 and 475°C for 1 h. The maximum load was 30 mN.

3.2. Young's modulus

The Young's modulus of Base glass and glass-ceramics was estimated from nanoindentation tests. The load/unload displacement curves for Base glass and a transparent glass-ceramic are shown in Fig. 4. It is well known that the Young's modulus of specimen

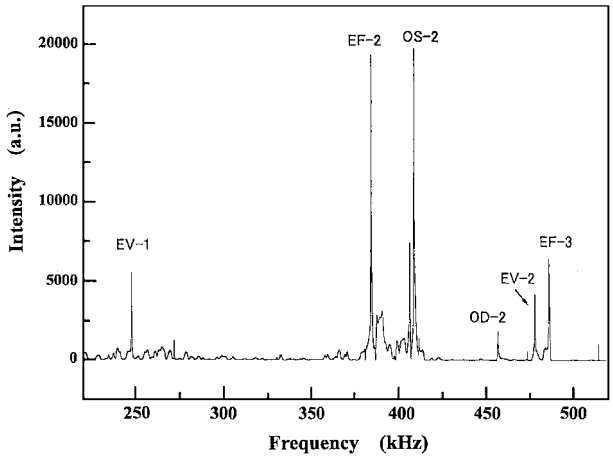

Figure 5 Cube resonance spectrum at room temperature for the Base glass ($15K_2O \cdot 15Nb_2O_5 \cdot 70TeO_2$) . The corresponding vibrational modes are also shown.

in the nanoindentation test is obtained in the form of the reduced modulus E_r, and a reduced modulus is expressed by Equation 2 [9].

$$\frac{1}{E_r} = \frac{(1-\nu^2)}{E} + \frac{(1-\nu_i^2)}{E_i} \tag{2}$$

where E and ν are Young's modulus and Poisson's ratio for the specimen and E_i and ν_i are the same parameters for the indenter. In this study, a diamond Vickers indenter was used, and the elastic parameters for diamond are $E_i = 1140$ GPa and $\nu_i = 0.07$ [10]. In order to estimate the Young's modulus of a specimen, the value of Poisson's ratio is needed. The Poisson ratio of Base glass was measured from a cube resonance method with the frequencies of 0.2–1 MHz, in which the sample size was $3.85 \times 3.85 \times 3.85$ mm [11, 12]. The cube resonance spectrum for Base glass is shown in Fig. 5, and the value of $\nu = 0.24$ was obtained. This value is well consistent with those in various glasses [13–15]. We tried to estimate the Poisson's ratio for the glass-ceramics, but sizable cubic samples could not be obtained because of the crack formation in large sizable glass-ceramics during heat-treatments. It is well known that the Poisson's ratio of oxide crystalline materials are usually 0.2–0.3 [13]. In the present study, therefore, the Young's modulus of the glass-ceramics was calculated by assuming the Poisson's ratio of $\nu = 0.24$, and the values are shown in Fig. 6. Base glass has $E = 54.7$ GPa, being typical one for TeO_2-based glasses [16]. On the other hand, the glass-ceramics have higher Young's moduli of $E = 71.6$–82.9 GPa. It should be pointed out that the increase in Young's modulus is not monotonous against the increase in the heat-treatment temperature. This behavior is similar to that in the Vickers hardness, but a slight decrease in E is observed at the transformation stage from phase I to phase II. At this moment, the mechanism of the transformation from phase I to phase II has not been clarified. But, it is considered from Fig. 2 that large atomic rearrangements occur at the transformation stage. In such a transformation stage, atomic arrangements might be considerably disorder-like, giving a decrease in Young's modulus.

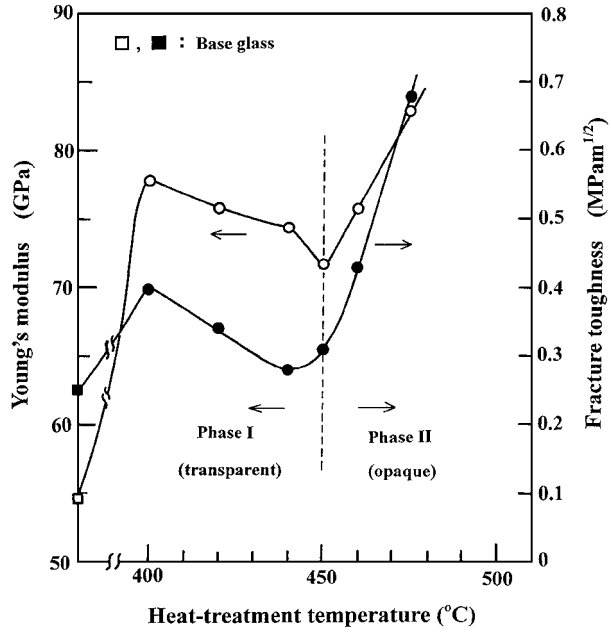

Figure 6 Young's modulus and fracture toughness at room temperature for the Base glass and glass-ceramics ($15K_2O \cdot 15Nb_2O_5 \cdot 70TeO_2$) obtained by heat-treatments at 400–475°C for 1 h.

The elastic recoveries after unloading in nanoindentation tests were estimated to be 44% for Base glass, 44% for the transparent glass-ceramic and 38% for the opaque glass-ceramic. These results suggest that a plastic deformation occurs easily even in transparent nanocrystalline glass-ceramics under the applied load of 30 mN, implying that the interaction among nanocrystalline particles is not so strong. It is of particular interest to examine the applied load dependence of elastic recovery, and such a study is now under consideration.

As described in this section, sizable cubic glass-ceramics (e.g. $5 \times 5 \times 5$ mm) could not be obtained easily because of the crack formation during cooling after heat-treatment. Since the thermal expansion coefficient α of TeO_2-based glasses are generally much large compared with conventional silicate glasses, the generation of internal stress would be a serious problem for the preparation of TeO_2-based glasses with large sizes. If a temperature gradient ΔT exists in a glass piece, internal stress occurs. The generated internal stress σ in glass is proportional to the Young's modulus and thermal expansion coefficient and can be estimated using Equation 3 [17]:

$$\sigma = \frac{E\alpha}{1-\nu}\Delta T = \varphi \Delta T \tag{3}$$

where φ is called specific thermal tension and is a characteristic parameter for a given glass. The estimated values of φ for Base glass and a transparent nanocrystalline glass-ceramic are 1.12 and 1.24 N mm^{-2}K^{-1}, respectively. Generally, silicate and borosilicate glasses have $\varphi = 0.7$–0.8 N mm^{-2}K^{-1} and lanthanum oxide borosilicate glasses show high values of $\varphi = 0.9$–1.2 N mm^{-2}K^{-1} [17]. The values of $\varphi = 1.12$ and 1.24 N mm^{-2}K^{-1} estimated here are, therefore, regarded as large ones, maybe giving the difficulty for large size TeO_2-based glasses and glass-ceramics.

3.3. Fracture toughness

The values of characteristic crack length, C, in Vickers indenter tests gives information on the resistance to fracture. Fracture toughness, K_c, which is a measure of the resistance to fracture, is expressed by the following Equation 4:

$$K_c = \frac{P}{\beta_o C^{3/2}} \tag{4}$$

β_o is a function of Young's modulus E and hardness H_v, and many models for the estimation of β_o have been proposed [18]. The following equation has been recommended by Japanese Industrial Standards (JIS) for ceramics [19]:

$$K_c = 0.018\left(\frac{E}{H}\right)^{1/2}\left(\frac{P}{C^{3/2}}\right) \tag{5}$$

Equation 5 is almost the same as that proposed by Anstis *et al*. [20]. It was found that the relation between P and C given by Equations 4 and 5, i.e. $C \propto P^{2/3}$, is well hold in Base glass and glass-ceramics. Using the values of Vickers hardness and Young's modulus, K_c values were determined, and are given in Table I and Fig. 6. The fracture toughness of Base glass is $K_c = 0.24$ $MPam^{1/2}$. This small value demonstrates that the tellurite glass of $15K_2O \cdot 15Nb_2O_5 \cdot 70TeO_2$ is mechanically very fragile, as already proposed by Watanabe *et al*. [3]. As seen in Table I, the glass-ceramics have the fracture toughness of 0.40–0.68 $MPam^{1/2}$, meaning that the fracture toughness is improved due to crystallization. The increase in fracture toughness is not monotonous against the increase in the heat-treatment temperature, as similar to the behaviors of Vickers hardness and Young's modulus. The results on the fracture toughness shown in Fig. 6 also suggest that the interaction among nanocrystalline phase I in transparent $15K_2O \cdot 15Nb_2O_5 \cdot 70TeO_2$ glass-ceramics is not so strong.

It is known that there is a good correlation between Young's modulus and fracture toughness in glasses and polycrystalline ceramics as shown in Fig. 7 [21]. The data obtained in the present study for Base glass and glass-ceramics are also plotted in Fig. 7. It is seen that the relation between E and K_c in TeO_2-based glass and glass-ceramics is included in the category of other glass and ceramics. This correlation is important to the design of TeO_2-based materials with high fracture toughness. That is, in TeO_2-based glasses and glass-ceramics, a key point to improve mechanical properties is to find effective elements giving large Young's modulus. In this connection, the study of mechanical and elastic properties of rare-earth doped or containing TeO_2-based materials might be valuable.

According to the fracture mechanics, the relationship between fracture toughness and Young's modulus is expressed by the following equation [22]:

$$K_c = \sqrt{\frac{2E\gamma_f}{1-\nu^2}} \tag{6}$$

where γ_f is the fracture surface energy. The fracture surface energy is termed as the energy associated with

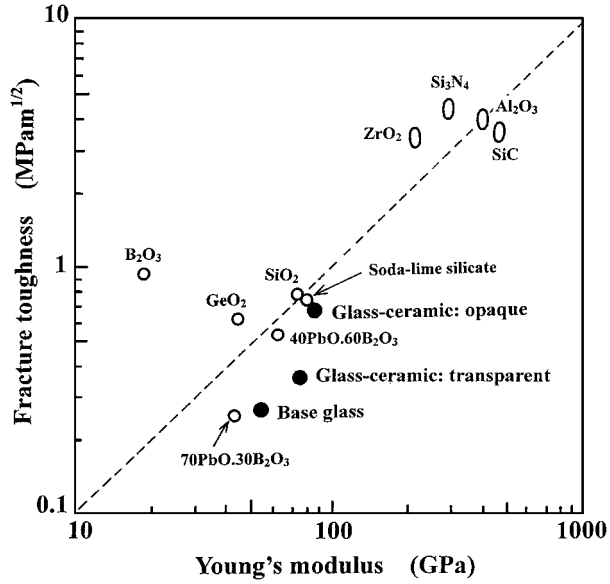

Figure 7 Relationship between Young's modulus and fracture toughness at room temperature for Base glass ($15K_2O \cdot 15Nb_2O_5 \cdot 70TeO_2$), transparent and opaque glass-ceramics. The data for other glasses and ceramics are included [21].

surface formation during fracture, and thus it controls the fracture process and is important in understanding the underlying mechanism affecting the fracture of solid materials [23], although it is recognized that the fracture surface energy measured experimentally is an effective fracture surface energy and does not directly correspond to the thermodynamic surface free energy. Wiederhorn [23] estimated the fracture surface energy of some silicate glasses using the double cantilever cleavage method. For example, the fracture surface energy of soda-lime silicate glass in an atmosphere of dry nitrogen is 3.8 Jm^{-2}. Equation 6 has been used to estimate the fracture surface energy of phosphate glasses, phase-separated glasses and $MgAlO_4$ single crystal [24–26]. In this paper, we estimated the fracture surface energies of TeO_2-based glasses and glass-ceramics using Equation 6. The values of $\gamma_f = 0.5$ Jm^{-2} for Base glass, $\gamma_f = 0.7$ Jm^{-2} for transparent nanocrystalline glass-ceramic (420°C, 1 h), and $\gamma_f = 2.6$ Jm^{-2} for opaque glass-ceramic (475°C, 1 h) were obtained. It is clear that the fracture surface energies of TeO_2-based glass and glass-ceramics are extremely small compared with other conventional glasses (generally around $\gamma_f = 5$ Jm^{-2}), indicating again that TeO_2-based glasses are fragile.

3.4. Brittleness

Since the so-called "brittleness" of glass and glass-ceramics, resulting in a high susceptibility to catastrophic failure, is major disadvantages that limit their use in various technical applications, it is important to understand their brittleness and to draw effective factors for materials designs with low brittleness. As indicated in the previous sections, it is considered that TeO_2-based glass and transparent nanocrystalline glass-ceramics would be brittle. In this section, we try to evaluate quantitatively the brittleness of our samples. Lawn and Marshall [27] have proposed a useful

approach for the quantification of the brittleness, in which a simple index of brittleness B is derived in terms of hardness H and Vickers indentation fracture toughness K_c:

$$B = \frac{H}{K_c} \tag{7}$$

Generally, B values for ceramic materials and glasses are varying in the range $\sim 1\ \mu m^{-1/2}$ to $13\ \mu m^{-1/2}$ [28]. The values of B in Base glass and glass-ceramics were estimated using Equation 7 and using the data of H_v and K_c. The results are given in Table I. Base glass has a large brittleness of $B = 11.6\ \mu m^{-1/2}$. The transparent nanocrystalline glass-ceramics have also large brittlenesses of 11.3–13.5 $\mu m^{-1/2}$, suggesting again that the interaction among nanocrystalline particles is not so strong. It is noted that the opaque glass-ceramics consisting of phase II exhibit relatively low brittleness, for example, the glass-ceramic heat-treated at 475°C has $B = 6.6\ \mu m^{-1/2}$.

The C/a ratio in Vickers indentation test is also an important parameter for the evaluation of brittleness, because it is related to the ratio of hardness and fracture toughness. Recently, Sehgal *et al*. [28, 29] have shown that the brittleness index B for various glasses can be obtained readily by measuring the C/a ratios in Vickers indentation patterns. The equation derived by Sehgal *et al*. [28, 29] on the basis of hardness and Vickers fracture toughness relationship and validated for glass-ceramics by Boccaccini [30] expresses the brittleness as:

$$B = \alpha_0^{-3/4} H^{3/4} E^{-1/2} \gamma^{-1} P^{-1/4} \left(\frac{C}{a}\right)^{3/2} \tag{8}$$

where γ is an empirical dimensionless parameter, which is often determined by experimental calibration. For silicate glasses the value of $\gamma = 18$ has been proposed by Sehgal *et al*. [28, 29], and for SiO_2-based glass-ceramics (Silceram glass-ceramics) Boccaccini [30] has proposed the value of $\gamma = 25$. It is of interest to check whether the above relation can extend to tellurite glasses and glass-ceramics. It was found that the value of $\gamma = 18$ can reproduce very well for almost transparent and opaque glass-ceramics as shown in Table I. It should be pointed out that this value is the same as that for glasses proposed by Sehgal *et al*. [28, 29]. Recently, non-conventional glasses such as TeO_2-based and Bi_2O_3-based glasses absorb much interest because they exhibit excellent optical properties and are excellent host materials for rare earth doping. For such fragile glass-forming systems, it is extremely important to clarify mechanical and elastic properties. It is strongly desired to check the validity of Equation 8 for such optical functional glasses with various compositions.

4. Conclusion

The information on the mechanical and elastic properties of TeO_2-based glasses and glass-ceramics is lacking compared to the study of their structure, optical and thermal properties. In this study, we examined various mechanical and elastic properties for the glass and glass-ceramics of $15K_2O \cdot 15Nb_2O_5 \cdot 70TeO_2$ using Vickers indentation and nanoindentation tests. For transparent nanocrystalline glass-ceramics, Vickers hardness, Young's modulus and fracture toughness became large compared with the precursor glass, but the fracture surface energy, brittleness and elastic recovery after unloading are almost the same as those of the precursor glass. It is considered that the interaction among nanocrystalline particles is not so strong and weak Te-O bond strength still affect strongly some mechanical and elastic properties in nanocrystalline TeO_2-based glass-ceramics. It was found that opaque glass-ceramics obtained by heat-treatment at 475°C have much better mechanical and elastic properties. It is desired to study mechanical and elastic properties of other TeO_2-based glass-ceramics and to draw general features for transparent nanocrystalline glass-ceramics.

Acknowledgements

This work was supported from the Grants of KAWASAKI STEEL 21st Century Foundation, the Ookura Kazuchika Memorial Foundation, and the Grant-in-Aid for Scientific Research from the Ministry of Education, Science, Sports and Culture, Japan. The authors thank Dr. Hidetoshi Saito, Nagaoka University of Technology, for the use of nanoindentation equipments.

References

1. J. S. WANG, E. M. VOGEL and E. SNITZER, *Opt. Mater.* **3** (1994) 187.
2. S. H. KIM and T. YOKO, *J. Amer. Ceram. Soc.* **78** (1995) 1061.
3. T. WATANABE, Y. BENINO, K. ISHIZAKI and T. KOMATSU, *J. Ceram. Soc. Japan* **107** (1999) 1140.
4. K. SHIOYA, T. KOMATSU, H. G. KIM, R. SATO and K. MATUSITA, *J. Non-Cryst. Solids* **189** (1995) 16.
5. H. G. KIM, T. KOMATSU, K. SHIOYA, K. MATUSITA, T. TANAKA and K. HIRAO, *ibid.* **208** (1996) 303.
6. T. KOMATSU, H. G. KIM and H. OISHI, *Inorg. Mater.* **33** (1997) 1069.
7. H. OISHI, Y. BENINO and T. KOMATSU, *Phys. Chem. Glasses* **40** (1997) 1069.
8. T. KOMATSU, Y. BENINO and R. SAKAI, *J. Japan Inst. Metals* **62** (1998) 1055.
9. W. C. OLIVER and G. M. PHARR, *J. Mater. Res.* **7** (1992) 1564.
10. R. Y. LO and D. B. BOGY, *ibid.* **14** (1999) 2276.
11. H. H. DEMAREST, JR, *J. Acous. Soc. Am.* **49** (1971) 768.
12. T. GOTO and N. SOGA, *J. Ceram. Soc. Japan* **91** (1983) 35.
13. W. D. KINGERY, H. K. BOWEN and D. R. UHLMANN, "Introduction to Ceramics" (John Wiley & Sons, New York, 1976) p. 770.
14. T. HANADA, N. SOGA and M. KUNUGI, *J. Ceram. Soc. Japan* **81** (1973) 481.
15. D. S. SANDITOV and S. SH. SANGADIEV, *Glass Phys. Chem.* **24** (1998) 525.
16. S. INABA, S. FUJINO and K. MORINAGA, *J. Amer. Ceram. Soc.* **82** (1999) 3501.
17. H. BACH and N. NEUROTH, "The Properties of Optical Glass" (Springer, Berlin, 1995) p. 182.
18. C. B. PONTON and R. D. RAWLINGS, *Mater. Sci. Tech.* **5** (1989) 865.
19. Japanese Industrial Standards, Report 1607 (1990) p. 7.
20. G. R. ANTIS, P. CHANTIKUL B. R. LAWN and D. B. MARSHALL, *J. Amer. Ceram. Soc.* **64** (1981) 533.
21. N. SOGA, *J. Non-Cryst. Solids* **73** (1985) 305.
22. A. S. TETELMANN and A. J. MCEVILY, "Fracture of Structural Materials" (Wiley, New York, 1967) p. 50.
23. S. M. WIEDERHORN, *J. Amer. Ceram. Soc.* **52** (1969) 99.

24. M. ASHIZUKA, E. ISHIDA, S. UTO and R. C. BRADT, *J. Non-Cryst. Solids* **104** (1988) 316.
25. N. MIYATA and H .JINNO, *J. Mater. Sci.* **16** (1981) 2205.
26. R. L. STEWART and R. C. BRADT, *ibid.* **15** (1980) 67.
27. B. R. LAWN and D. B. MARSHALL, *J. Amer. Ceram. Soc.* **62** (1979) 347.
28. J. SEHGAL, Y. NAKAO, H. TAKAHASHI and S. ITO, 1 *J. Mater. Sci. Lett.* **14** (1995) 167.
29. J. SEHGAL and S. ITO, *J. Amer. Ceram. Soc.* **81** (1998) 2485.
30. A. R. BOCCACCINI, *J. Mater. Sci. Lett.* **15** (1996) 1119.

Received 8 August 2000
and accepted 13 June 2001